Stochastic Modeling for the Next Day Domestic Demand Response Applications

M. Tavakoli Bina, *Senior Member, IEEE*, and Danial Ahmadi

***Abstract*—Demand response (DR) refers to the consumers' activities for changing the load profile with the purpose of lowering cost, improving power quality or reliability of power system. Enhancement in participation of the DR is widely recognized as a profit-making pattern in distribution systems for both residential units (to increase their benefits) and distribution companies (DISCO) (to reduce their peak demand and costs). The target of this research is concentrated on proposing a *new strategy* for optimal scheduling of flexible loads for *the next day*. Then, the day ahead pricing (DAP) is modeled using the inclining block rates (IBR), assumed for retail electricity markets, to investigate the efficiency of the proposed strategy. At the same time, the appliances stochastic time of use (ASTOU) are taken into account in residential units for non-controllable part of the load during a day stochastically. Among five various copulas, the Gaussian copula (GC) function shows the best performance in modeling and estimation of non-controllable load consumption. Finally, simulations, performed with the GAMS, illustrate the effectiveness of the suggested approach which is formulated as a stochastic nonlinear programming (NLP) modeled by the GC. Notice that copulas use samples of real data gathered from residential units.**

***Index Terms*—Appliances stochastic time of use (ASTOU), day ahead DR strategy (DADRS), demand response (DR), GAMS, Gaussian copula, stochastic modeling.**

NOMENCLATURE

DR	Demand response.
DISC	Distribution companies.
ASTOU	Appliances stochastic time of use.
GC	Gaussian copula.
DAP	Day ahead pricing.
IBR	Inclining block rates.
NLP	Nonlinear programming.
Rho	Coefficient matrix.
ICDF/φ^{-1}	Inverse cumulative distribution function.
φ_m	m-dimensional standard multivariate normal distribution.
DADRS	Day ahead DR strategy.
AC	Air conditioner.
C	Copula functions.
EV	Electric vehicle.
TOU	Time of use.
WM	Washing machine.
DW	Dish washer.
MPF	Marginal price factor.
m	Number of random variables.
WRL	Weather related loads.
ECV	Energy consumption vector.
N	Scheduling horizon in energy consumption.
h	Time index.
ε	Factor of inertia.
ε_1	Equal to $(1-\varepsilon)^{-1}$.
η	Coefficient of performance.
λ	Control time period.
TC	Thermal conductivity.
t_m	Total thermal mass.
$te^h_{WL/TDR}$	Total required energy of all WRL/flexible loads at the hth hour.
$\theta^{in/out}_{h-1}$	Indoor/outdoor temperature at time $(h-1)$.
$e^{h,s_{Wk}}_k$	Consumed energy of appliance k in the hth time index s_{Wk} scenario.
$E^{ave,s_{Wk}}_k$	Average of daily demand for appliance k from WRL in s_{Wk} scenario.
m_0, m_1, m_2	Number of ASTOU, WRL, flexible loads.
te^h_{ASTOU}	Total energy for the operation of ASTOU in the hth hour.
e^h_j	Consumed energy of flexible loads, eu_j, during the hth time.
$e^h_{eu_j}$	Energy consumption of ASTOU, eu_j, in the hth time.
M_j	Total energy required for the operation of flexible load eu_j, per loading.
$[A_j, B_j]$	Period of time to plug in appliance eu_j.
$D^{\max\,/\,\min}_j$	Maximum/minimum hourly demand level of appliance eu_j.
A_f	Average frequencies of using ASTOU in a day.
$t_{tou/u}$	Time of use/usage time of ASTOU.
T^z_s	The sth time of use the zth ASTOU in a residential unit.

Manuscript received December 16, 2013; revised January 03, 2014, May 10, 2014, August 08, 2014, and September 23, 2014; accepted December 06, 2014. Paper no. TPWRS-01488-2013.

The authors are with the Electrical Engineering Faculty, K. N. Toosi University of Technology, Tehran 16314, Iran (e-mail: tavakoli_bina@ieee.org; ahmadi.danial@ee.kntu.ac.ir).

Color versions of one or more of the figures in this paper are available online at http://ieeexplore.ieee.org.

Digital Object Identifier 10.1109/TPWRS.2014.2379675

D_s^z	Usage time of the zth ASTOU in the sth time of use.
$e_z^{h/ave,s_{Az}}$	Consumed energy in the hth hour for appliance z (ASTOU) in s_{Az} scenario.
$E_z^{ave,s_{Az}}$	Average daily energy for appliance z from the ASTOU in s_{Az} scenario.
c^n	Marginal pricing in retail markets.
C^h	Cost of energy in the hth hour.
E_{Total}^h	Total demand of end users in the hth hour.
E_{day}	Total demand of flexible loads for 24 h.
C_{Total}	Total daily payment by user.
E_{ave}^h	Average of daily demand in different scenarios.
θ_i^j	Temperature of the ith hour in the jth day.
$\theta_f^{z_1}$	Temperature at time f of the z_1th selected day.
e_{AC}^h	AC energy consumption at time h.
$\boldsymbol{\tau}$	Kendall's rank correlation matrix.

I. Introduction

THE increasing peak demand causes shortage on the available power generation, congestion of transmission and distribution infrastructure as well as growth in the price of energy in the wholesale markets [1]. Meeting the peak demand is further associated with the potential transformer overloads, undue circuit faults and risk of forced outages. In recent years, the demand response (DR) has been proposed in smart grids to reduce the peak demand. The DR is defined as "changes in electric usage by end users from their normal consumption patterns in response to changes in the price of electrical energy over time, or incentive payments designed to induce lower electrical energy use at times of high wholesale market prices or when the system reliability or power quality is jeopardized" [2]. According to this definition, efficient use of the DR strategies plays an important role in balancing the supply and demand; especially during the peak periods. Hence, the DR can increase the reliability and efficiency through shifting and shedding the peak demand [3]–[5].

Three types of DR automation levels exist for residential units; namely, manual, semi-automated and fully-automated DR [6]. The manual DR is an ineffective automation level because of consumer inertia, lack of end users knowledge on how to respond as well as in time programming of the electrical usage by the consumers. Moreover, most of fully-automated DR strategies are focused on scheduling the present time of use (TOU) with critical peak pricing or real-time pricing programs. This type of DR automation requires numerous equipment (smart metering, control and communication infrastructure) as well as particular arrangements for controlling flexible loads. Therefore, fully-automated DR strategies are expensive and complicated in implementation. Nevertheless, researchers have presented different algorithms and strategies related to the fully-automated DR over the past several years in the literatures [7]–[13].

In contrast, performing a semi-automated DR requires an event notification by the system manager through the internet

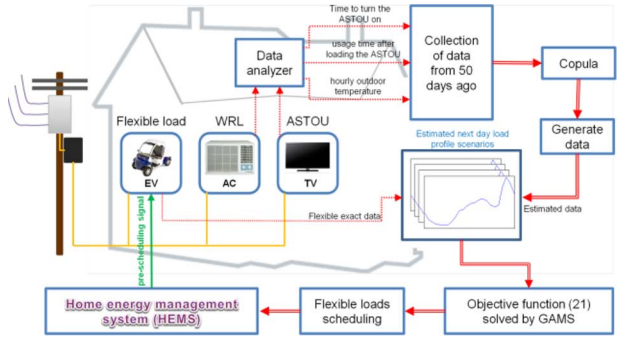

Fig. 1. Outline of the research work performed in this paper, including the home appliances, estimation and generation of next day load profile scenarios, finding out the optimized scenario and scheduling flexible loads.

for the consumer in advance (a few hours). In comparison with a fully-automated DR, a semi-automated DR needs less equipment, while it is much cheaper. In practice, a semi-automated DR can result in the same outcomes as those of fully-automated DR by using an appropriate strategy to control flexible loads.

This paper presents a new semi-automated proposal on the day ahead demand response strategy (DADRS) to decrease the peak demand and increase the benefits of residential units. Generally, most of the DR-related methods, proposed previously, investigated on the present TOU [7]–[13]. However, only a few papers focus on scheduling flexible loads for the next day. Moreover, several TOU or day ahead strategies have been focused on controlling flexible loads such as washing machine (WM), dish washer (DW), electrical vehicle (EV), and so on [7], [8]by assuming a certain load profile for non-controllable part. This implies ignoring the necessity of modeling non-controllable uncertain loads (e.g., TV and PC) in establishing a precise profile. This paper, however, proposes a novel model for energy consumption of the appliances stochastic time of use (ASTOU) using copula. Moreover, the consumed demand for weather related loads (WRL) is yet to be stochastically studied in literatures as the fixed part of the load [e.g., air conditioner (AC)]. Clearly, the error in forecasting temperature has significant impact on the load forecasting of the WRL [14], [15]. Fig. 1 provides a clear picture on how this research is arranged. Samples of various customer loads are taken, including both non-controllable loads (the ASTOU and the WRL) and flexible loads. The required exact data are gathered over 50 days as the basis for the analysis. Then, a copula function is used for estimating rank correlation of the gathered samples random variables as a multivariate distribution function for both the WRL and the ASTOU. Consequently, new scenarios can be generated using the estimated multivariate distribution function. It should be noted that the new generated scenarios are useful for the stochastic analysis. Thus, different scenarios are fed to the GAMS to solve an optimization problem. The GAMS eventually provides the required operating commands for the flexible loads through the home energy management system (HEMS). Therefore, this paper introduces *the DADRS* that focuses on *controlling flexible loads*; taking into account both the *energy consumption* of *the ASTOU* (e.g., TV and PC) and estimating *the WRL* energy consumption by including error in forecasting temperature. This paper examines five different copulas using the real data in

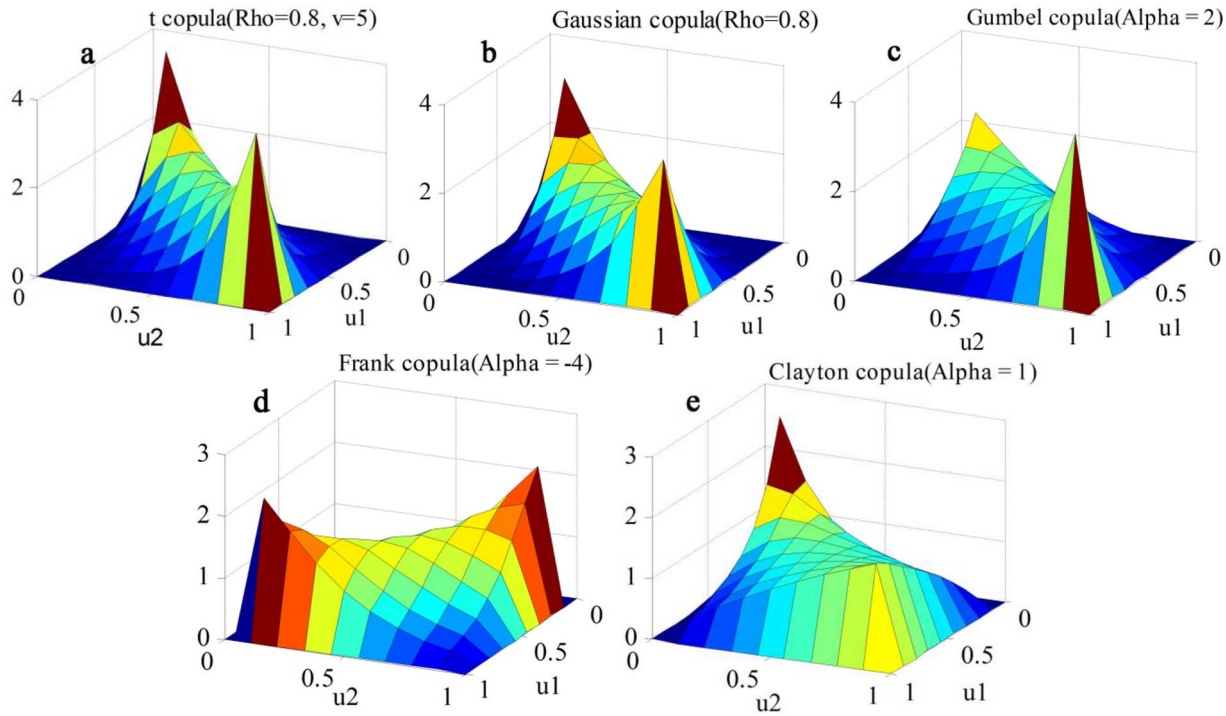

Fig. 2. Sample of different bivariate copula functions (a): t copula ($\mathbf{Rho} = 0.8, \boldsymbol{v} = 5$); (b): Gaussian copula ($\mathbf{Rho} = 0.8$); (c): Gumbel copula ($\boldsymbol{\alpha} = 2$) (d): Frank copula ($\boldsymbol{\alpha} = -4$); (e): Clayton copula ($\boldsymbol{\alpha} = 1$).

which an *elliptical copula* (the GC) was selected for modeling the ASTOU. The proposed DADRS with stochastic process is solved by the GAMS. The outcomes will help distribution companies (DISCO)/aggregators to decrease their peak demand as well as users' payment in retail markets. Finally, simulations are presented in which 100 home consumers are considered under three different scenarios; the case study is directed towards the suggested estimation of the WRL and the ASTOU as well as the DR for the flexible loads. This research also assumes the DAP with the IBR model for the retail electricity market. Simulations show that the suggested estimations of energy consumption of the WRL and the ASTOU in scheduling flexible loads contributes to further reduction in both the peak demand and the energy cost. In brief, contributions of this research are modeling residential non-controllable loads that are uncertain such as TV, PC, lighting, and the WRL using the GC along with proposing a strategy in controlling flexible load for the next day in a residential unit using the following steps:

- Samples of various ASTOU and WRL appliances were gathered over fifty days as the real dataset.
- Each ASTOU and WRL appliance is separately modeled using a selected copula function.
- Generating a dataset of size N according to the modeled copula for each appliance.
- Converting N created scenarios for each ASTOU and/or WRL appliance into N load profiles for stochastic analysis.
- Requesting the parameters of the flexible loads from 100 residential units.
- Applying the gathered flexible loads together with simulated scenarios (profiles) of the ASTOU and the WRL to the GAMS for stochastic analysis using the proposed objective function (17).
- The GAMS eventually provides the required operating commands for the flexible loads through the home energy management system (HEMS). The outcomes will help distribution companies (DISCO)/aggregators to decrease their peak demand as well as users' payment in retail markets.

II. Overview on Application of Copulas

Here it is described benefits of copulas for data creation. Copulas are functions that join or couple multivariate distribution functions to their one-dimensional marginal distribution functions. As shown in Fig. 1, the main task of copula is to estimate a multivariate distribution function based on the marginal and rank correlation of the taken sample data. Then, various scenarios are generated according to the estimated multivariate distribution function. In mathematical terms, copulas are multivariate distribution functions (C) of m random variables whose one-dimensional marginal distributions are uniform within the interval $[0, 1]^m$, where m is the number of dependent outcomes that should be modeled. It can be shown from definition that copulas are capable of describing nonlinear dependence among multivariate data independent from their marginal probability distributions [16]. Copulas can also serve as a powerful tool for both modeling and simulating nonlinearly-interrelated multivariate data, and uniform continuity and existence of all partial derivatives [18]. Some samples of t, Gaussian, Gumbel, Frank, and Clayton copulas which are known as the Archimedean and Elliptical copulas are illustrated in Fig. 2 in bivariate form.

A. Why Copula?

In brief, the most interesting advantage of copula functions is their capability in estimating marginal and rank correlation of samples of random variables, joining these distribution functions to their one-dimensional marginal distributions (see detailed description on definitions and properties in [16]–[18]). So, the modeling principles of copulas allow easy modeling and estimation of multivariate distribution function. In other words, compared to other estimating methods, copula inter-relates nonlinearly multivariate data. The following steps are taken to generate data with copula:

- fitting an appropriate marginal distribution, probability distribution function (PDF), to each variable according to the real dataset;
- obtaining the CDF of each PDF worked out in the previous step in order to transform actual random variables to the uniform distribution (i.e., $[0, 1]$);
- calculating Kendall's rank correlation $\boldsymbol{\tau}$ using the CDF; then the characteristics of the copula (**Rho**) is calculated according to the employed copula function;
- generating datasets of size N on a unit hypercube $[0, 1]^m$ (m is the number of random variables) with uniform marginal probability distributions according to the calculated **Rho**;
- applying inverse CDF (ICDF) to transform the generated uniform dataset of size N to an actual dataset of size N. This created dataset has the same characteristics as those of gathered real data.

Sometimes the number of initial real dataset cannot be extended as many as required in practice. For example, the number of taken samples from the owner of the PC is limited due to various economical, practical and social restrictions. It should be noted that estimating the required demand of the PC in the next day could help end user to provide and optimally pre-schedule flexible loads. However, limited number of samples taken from the PC has to be expanded in order to enable the customer to estimate the load profile for the PC.

Here it is demonstrated a simulation in which the samples of the PC in 50 days are available as exact data; once copula estimates 20 sets of 50 data from the exact data, and another time 1000 data are estimated directly from 50 exact data. Simulations are shown in Fig. 3(a)–(c), in which 1000 dataset are compared correspondingly for the two ways of data estimation. Both the estimated data and their PDF confirm that the two ways of estimating with copula are quite the same.

B. Comparing Copula With Traditional Models

Unlike copula, traditional models (e.g., normal and log-normal) ignore dependence among random variables. To compare these traditional models with copula, assume a real dataset includes 1000 *exact* datasets gathered from 1000 TVs (these data were collected from a national organization), each containing four variables (see detailed definitions in Section III-A within Section III). These datasets were used to work out the exact 24-h load profiles for 1000 TVs as shown in Fig. 4(a)–(c) by blue curves. This load profile is regarded as the *exact reference* that estimates of other modeling methods are compared with. Fig. 4(a) depicts 24-h load profiles, while

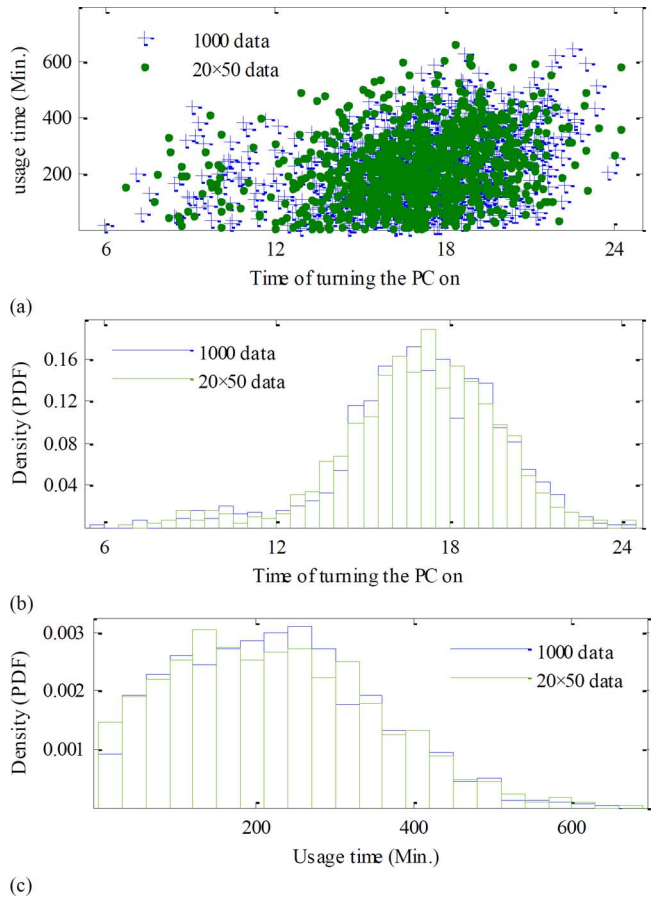

Fig. 3. Copula estimates 20 sets of 50 data (in green) and one set of 1000 data (in blue) from 50 exact data: (a) estimated data, (b) the PDF of the estimated time of turning the PC on, and (c) the PDF of estimated usage time of turning the PC on.

Fig. 4(b) and (c) illustrates division of Fig. 4(a) into two 12-h load profiles in order to get a better visual resolution.

Then, assume 50 exact datasets from 50 TVs are applied to two traditional models (normal and log-normal) as well as copula to *estimate* 1000 datasets. Again, these generated 1000 datasets using normal, log-normal and copula were converted into three load profiles. Green curves in Fig. 4(a)–(c) demonstrate the load profile based on 1000 estimated datasets using *copula*, red lines are the load profile derived from 1000 estimated datasets using *normal distribution* and black lines illustrate the load profile rooted on 1000 estimated datasets using *log-normal distribution*.

It can be seen from Fig. 4 that copula predicts a much closer load profile to the exact load profile compared to those of traditional models. To get a meaningful comparison, performances of copula, normal and log-normal distributions are tested in this paper using the well-known mean absolute percentage errors (MAPE) as follows ([19]):

$$MAPE = \left[\frac{1}{24}\sum_{i=1}^{24}\left|\frac{d_i - P_i}{d_i}\right|\right] \times 100 \qquad (1)$$

where d_i and P_i are the exact reference and predicted demand at the ith hour, respectively. The MAPE of the three prediction models are worked out in Table I for the three pictures in

TABLE I
MAPE AND ABSOLUTE ERROR RELATED TO ESTIMATED LOAD PROFILES OF 1000 TVS (NORMAL, LOG-NORMAL DISTRIBUTIONS, AND COPULA) WITH RESPECT TO THE EXACT REFERENCE (SEE FIG. 4)

Data Creation Method	MAPE%			Absolute Error: Fig. 4 (b) (with respect to the actual data)			Absolute Error: Fig. 4 (c) (with respect to the actual data)		
	Fig. 4 (b)	Fig. 4 (c)	Fig. 4 (a)	Maximum (kW)	Minimum (kW)	Average (kW)	Maximum (kW)	Minimum (kW)	Average (kW)
Univariate Normal	241.68	12.03	126.86	23.20	1.43	7.18	18.43	3.47	10.65
Univariate Log-Normal	700.23	15.07	357.65	18.65	3.92	7.68	20.88	3.54	13.11
Copula	22.13	3.19	12.66	8.77	0.07	1.52	5.83	0.10	3.13

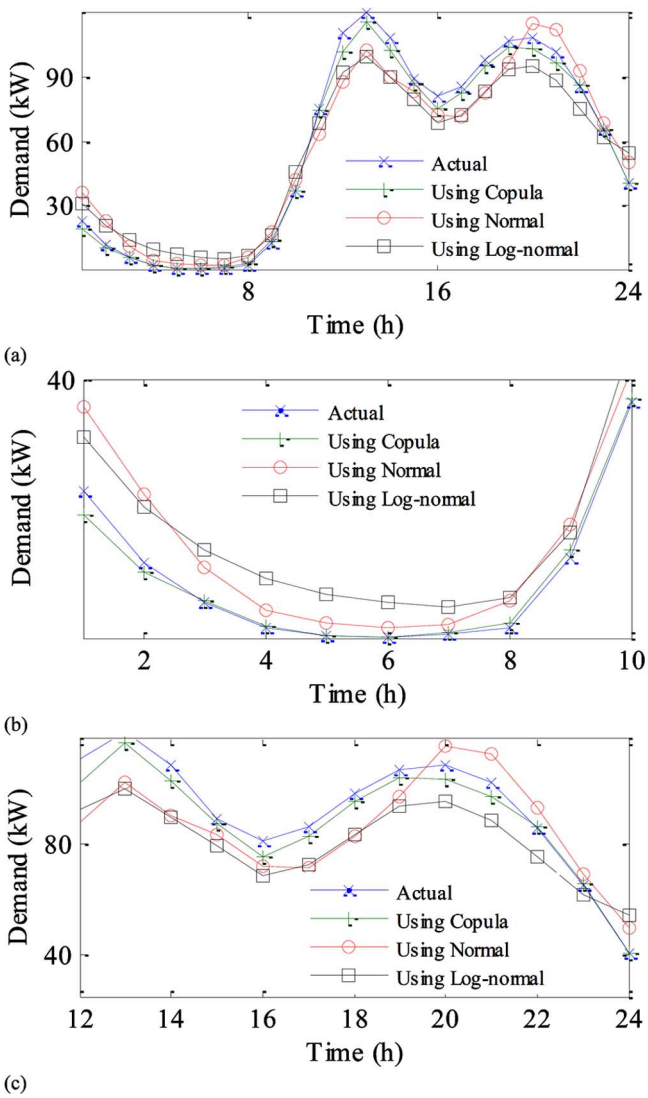

Fig. 4. Load profile of 1000 TVs based on actual, simulated data using copula, normal, and log-normal between (a): 00:00 a.m. to 24:00 p.m.; (b): 00:00 a.m. to 10:00 a.m.; (c): 12:00 a.m. to 24:00 p.m.

Fig. 4. It is clear that copula performs much better than traditional normal and log-normal models. Table I also shows the absolute errors (maximum, minimum and average errors) in kW for the two divided load profiles in Fig. 4(b) and (c) with respect to the exact reference. Both the MAPE and absolute errors in Table I confirm copula as the best statistical distribution to model the load profile for TV.

TABLE II
AIC AND HQIC INFORMATION CRITERIA FOR MODELING THE TIME OF TURNING THE PC ON AND USAGE TIME OF IT

	AIC	HQIC
T	3.71	7.43
Frank	2.86	6.58
Gumbel	2.22	5.94
Clayton	1.67	5.39
Gaussian	0.74	2.6

C. Selection of a Proper Copula

Here five different copulas are examined in order to select the best one in creating large datasets for both PC and TV. These copulas are nominated from the Elliptical (Student's t and Gaussian) as well as the Archimedean (Gumbel, Frank, and Clayton) that are more common in this area. Two assessing relationships are defined in [20]and [21]to compare the capability of a given copula in data creation; the Hannan-Quinn Information Criterion (HQIC) and Akaike Information Criterion (AIC). A copula associated with the *smallest* value of the selected information criterion, is considered to be the best-fit copula [20]. Tables II and III show values of the AIC and HQIC information (calculated with MATLAB) for the created large datasets (using the algorithm in Section II-A) from exact data related to PC (1000×2 from 50×2) and TV (1000×4 from 50×4), respectively. It can be seen from Tables II andIII that the GC is the best copula for modeling both the PC and TV according to the AIC and HQIC.

The GC or elliptical copula is the most familiar among all copulas and is distributed over the unit cube $[0,1]^m$. The m-dimensional GC is defined as follows:

$$C^d(u_1,u_2,\ldots,u_d;\mathbf{Rho}) = \varphi_d(\varphi^{-1}(u_1),\varphi^{-1}(u_2),\ldots,\varphi^{-1}(u_d);\mathbf{Rho}) \quad (2)$$

where $\varphi^{-1}(.)$ is the inverse cumulative distribution function (ICDF) of a standard normal distribution function $\varphi(.)$; and $\varphi_m(.;\mathbf{Rho})$ is the m-dimensional standard multivariate normal distribution function with mean vector zero and covariance matrix equal to the correlation matrix, **Rho** [16].

In what follows, the ASTOU are modeled using bivariate and multivariate GC. In this case, energy consumption of flexible

TABLE III
AIC AND HQIC INFORMATION CRITERIA FOR MODELING THE TV

	AIC	HQIC
Gumbel	19.04	20.9
Clayton	16.06	17.92
Frank	12.58	14.45
T	-551.02	-538.07
Gaussian	-557.77	-546.66

loads (e.g., EVs) in the next day is optimally scheduled considering electrical energy consumption of WRL (e.g., AC) and ASTOU.

III. PROBLEM FORMULATION

Here appliances are categorized in an smart home and modeled for estimating their energy consumptions. This will then allow optimal scheduling of flexible loads in the next day. Equipment in smart homes can be divided into three categories; WRL, flexible loads and loads with uncertainty (the ASTOU that are related to the consumer behavior). The following section describes the proposed models. First, the consumed power of the ASTOU, such as TV and PC, is modeled using bivariate and multivariate GC. Further, an hourly electrical consumption is considered for the WRL, estimated based on the stochastic modeling using the GC. The goal is to improve the efficiency of the proposed DADRS.

A. Residential Loads

Assume a household customer is participated in the day ahead DR programming. In [8], an energy consumption vector is defined for each instrument, $\mathbf{ECV_{eu_i}}$, as follows:

$$\mathbf{ECV_{eu_i}} = \left[e^1_{eu_i}, e^2_{eu_i}, \ldots, e^N_{eu_i}\right], \quad i = 1, 2, \ldots, m_0 + m_1 + m_2 \tag{3}$$

where m_0, m_1, and m_2 are the number of ASTOU, the WRL, and flexible loads, respectively, $e^h_{eu_i}$ is the energy consumption of the appliance e_{u_i} at a certain hour $h \in \{1, \ldots, N\}$, and N is the scheduling horizon for energy consumption. Notice that N shows the number of hours ahead, which takes demand policies into account. In this paper, N is assumed to be 24 (hours) in order to cover scheduling horizon of a day.

1) Loads With Uncertainty: Both the ASTOU and the WRL were named as the loads with uncertain parameters in a residential unit. The error of forecasting weather can be modeled using the GC. Also, modeling energy consumption of the ASTOU and the WRL has an appropriate influence on scheduling flexible loads for the next day. Thus, it is necessary to model accurately the **ECV** of all home appliances for improving the next day DR.

a) Proposed Model for Energy Consumption of the ASTOU: Dependence structure of random variables is among the most interesting topics in recent years. Unlike the conventional approaches, copula theorem efficiently models the dependencies between random variables [16]. In [22], the GC is named as a popular family of copulas, where parameters of the GC function (**Rho**) can be estimated by means of Kendall's rank correlation ($\boldsymbol{\tau}$) ([17]) as follows:

T_1^z	D_1^z	T_2^z	D_2^z	...	T_{Ri}^z	D_{Ri}^z

Fig. 5. Proposed model for the ASTOU energy consumption.

$$\mathbf{Rho} = \sin\left(\frac{\pi}{2}\boldsymbol{\tau}\right), \ \boldsymbol{\tau}_{ij} \in [-1, 1]. \tag{4}$$

There are three important factors in order to model the **ECV** of the ASTOU with copula; these are the average frequency of using the ASTOU in 24 h (A_f), time of turning the ASTOU on (t_{tou}), and usage time after loading the ASTOU (t_u). Fig. 5 shows the required data for modeling the ASTOU energy consumption. Here R_i is the nearest rounded integer less than or equal to A_f, $z \in \{1, \ldots, m_2\}$, T_s^z and D_s^z are the sth time of turning on the zth ASTOU and its usage duration, respectively, ($s = \{1, \ldots, R_i\}$). To make the proposition more sensible, assume hourly consumed energy of a TV was monitored for 50 days; also, A_f and t_{tou} were collected. These gathered real data are used to model the **ECV** of the TV for the coming day by the multivariate GC. The average frequency of using the TV is $A_f = 2.3 (R_i = 2)$ in 24 h. Thus, parameters in Fig. 5 are restricted to T_1, D_1, T_2, and D_2, where these are the first and the second time of turning the TV on along with their usage times. Therefore, to estimate the load profile of the TV for the next day, the GC [defined in (1)]takes the dependencies of these four random variables into account to generate new data based on the available collected data. The parameter of the GC (**Rho**) can be estimated by means of an approximation to Kendall's rank correlation. This was done to obtain dependencies between the four parameters T_1, D_1, T_2, and D_2 as follows:

$$\mathbf{Rho} = \begin{bmatrix} 1.00 & 0.66 & 0.92 & -.50 \\ 0.66 & 1.00 & 0.74 & -.40 \\ 0.92 & 0.74 & 1.00 & -.62 \\ -.50 & -.40 & -.62 & 1.00 \end{bmatrix}. \tag{5}$$

The coefficient matrix (5) shows that the highest rank correlation is equal to 0.92 between T_1 and T_2. So, a nearly linear relationship can be seen in Fig. 6(b) between T_1 and T_2. For example, if the device is turned on for the first time in the early morning, it will be used most likely for the second time in the early afternoon or vice versa. Here it is explained a model in which a multivariate (four random variables) GC can be employed to generate different scenarios using the established correlations. These scenarios can be defined as the **ECV** for the considered TV as an ASTOU example. Hence, various scenarios were simulated using the developed multivariate GC (1000 scenarios) as the **ECV** for the TV (see Fig. 6). The generated **ECV** are useful for the stochastic process in the final proposed DADRS. The six pictures in Fig. 6 illustrate how much the generated 1000 scenarios are correlated according to dependence of two out of four variables. Notice that the

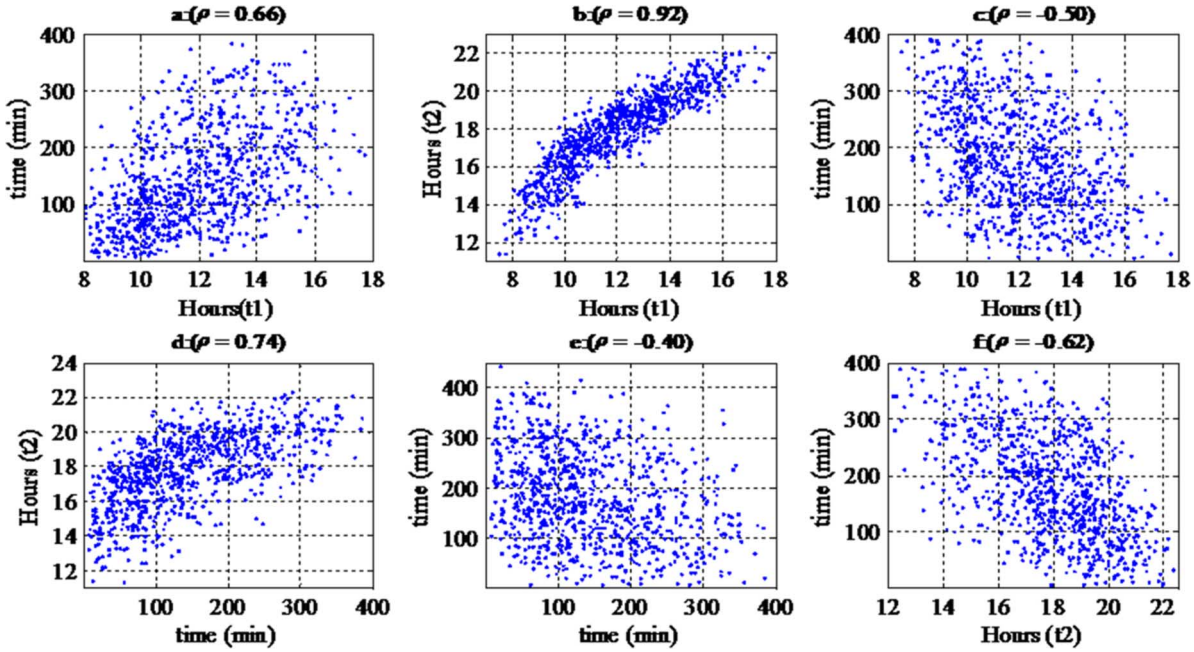

Fig. 6. One thousand different simulated scenarios for the TV electrical consumption as a visual demonstration of the data presented in (8); scattered plot of the simulated data for (a) T_1, D_1, (b) T_1, T_2, (c) T_1, D_2, (d) D_1, T_2, (e) D_1, D_2, and (f) T_2, D_2.

generated scenarios uphold the GC approximate correlations in (5).

The total demand for the operation of loads with uncertainty ($t_{e^h_{ASTOU}}$) that are estimated as a stochastic modeling by the GC at the hth hour ($h = 1, 2, \ldots, 24$) can be expressed as follows:

$$\begin{cases} te^h_{ASTOU}\left(e_1^{h,s_{A_1}}, e_2^{h,s_{A_2}}, \ldots, e_{m_0}^{h,s_{A_{m_0}}}\right) = \sum_{z=1}^{m_0} e_z^{h,s_{Az}} \\ E_z^{ave,s_{Az}} = \frac{1}{24}\sum_{h=1}^{24} e_z^{h,s_{Az}} \end{cases} \tag{6}$$

where $m_0 = 3$, $e_1^{h,s_{A1}} = e_{TV}^{h,s_{A1}}$, $e_2^{h,s_{A2}} = e_{PC}^{h,s_{A2}}$, and $e_3^{h,s_{A3}} = e_{Li}^{h,s_{A3}}$ are the ASTOU loads including TV, PC, and lighting, respectively, and $E_z^{ave,s_{Az}}$ is energy consumption and average daily demand of appliance eu_z at the hth hour and scenario s_{Az}.

b) Weather Related Loads (WRL): Generally, estimation of energy consumption of the WRL for hours ahead can be performed using mathematical formulation. At the same time, predicted weather conditions (e.g., temperature, lighting, and humidity) are the main collecting parameters affecting the WRL. The more accurate the prediction of weather conditions, the better it helps end users to satisfactorily predict WRL energy consumption. This would lead achieving a greater control on flexible loads. Thus, let te^h_{WL} be the total demand for the operation of all WRL at the hth hour ($h = 1, 2, \ldots, 24$) of the day ahead as follows:

$$te^h_{WL}\left(e_1^{h,s_{W_1}}, e_2^{h,s_{W_2}}, \ldots, e_{m_1}^{h,s_{Wm_1}}\right) = \sum_{k=1}^{m_1} e_k^{h,s_{Wk}} \tag{7}$$

$$E_k^{ave,s_{Wk}} = \frac{1}{24}\sum_{h=1}^{24} e_k^{h,s_{Wk}} \tag{8}$$

where $e_k^{h,s_{Wk}}$ and $E_k^{ave,s_{Wk}}$ are the consumed energy of appliance $k \in \{1, 2, \ldots, m_1\}$ at the hth hour, and the average daily demand of the kth appliance in scenario s_{Wk}. The WRL in a residential unit are refrigerators, freezers, water heaters and the AC. The proposed method can also be applied to the WRL for generating various scenarios; here scenarios are generated only for the AC ($e_1^{h,s_{W_1}} = e_{AC}^{h,s_{W_1}}$) as an example ($m_1 = 1$). Since prediction of temperature can be collected from meteorological agencies [23], weather prediction errors are assumed to be up to thirty percent (see [23]). This is considered in [23]for accurate prediction of outdoor temperature especially on rainy days. The energy consumption of the AC is obtained from (9) at the hth hour where plus and minus are applied to the heat and cool space-conditioning, respectively [15]:

$$\pm e^h_{AC} = \frac{TC.(\varepsilon_1\theta^{in}_h - \varepsilon\varepsilon_1\theta^{in}_{h-1} - \theta^{out}_{h-1})}{\eta} \tag{9}$$

where e^h_{AC} is the AC energy consumption in kW at the hth hour, ε is the factor of inertia, ε_1 is equal to $(1-\varepsilon)^{-1}$, θ^{h-1}_{in} and θ^{h-1}_{out} are the indoor and outdoor temperatures in °C at the $(h-1)$th hour, respectively, TC is the thermal conductivity in kW/°C, and η is the coefficient of performance. Note that η is equal to $e^{-\lambda.TC/tm}$, where λ is the controlling period (it is assumed $\lambda = 1$ h in this paper for the DR since the load is controlled hourly) and t_m is the total thermal mass in kWh/°C.

2) Flexible Loads: Assume the parameter $M_j (j \in \{1, \ldots, m_2\})$ is introduced as the total energy required per operation of the flexible appliance eu_j. Additionally, let $[A_j, B_j]$ denotes the starting and finishing times during which eu_j is plugged in by an end user. For example, energy consumption of a WM with warm setting is expressed by $M_j = 3.6$ kWh under a typical frontloading [8]. As another example, full charging of the battery of an EV can be scheduled by choosing $A_j = 8$ p.m. and $B_j = 6$ a.m. (early morning in the next day). Hence, the following relationship is considered for modeling

energy consumption of flexible loads when parameters A_j, B_j and M_j are determined by customers [8]:

$$M_j = \sum_{n=A_j}^{B_j} e^h_{eu_j}, \{\forall eu_j | [A_j, B_j] \in n, A_j < B_j\}. \quad (10)$$

Further, home instruments have special maximum and minimum hourly demand levels. Let us denote them by $D^j_{\max}$ and $D^j_{\min}$ for the appliance eu_j. For example, in [8], the pre-determined maximum power level for an EV is 3.3 kWh. Thus, these hourly demand levels are indicated by *residential units* for the day ahead DR programming as follows:

$$D^{\min}_j \le e^h_j \le D^{\max}_j, \quad h = A_j, A_{j+1}, \ldots, B_j \quad (11)$$

where e^h_j is the consumed energy of appliance eu_j during the region h. Moreover, the total demands for the operation of flexible loads at the hth hour (te^h_{TDR}) can be obtained as follows:

$$te^h_{TDR} = \left\{ \sum_{j=1}^{m_2} e^h_j \;\middle|\; \begin{array}{c} M_j = \sum_{h=A_j}^{B_j} e_{eu_j}, \\ D^{\min}_j \le e^h_j \le D^{\max}_j, h = A_j, \ldots, B_j \end{array} \right\} \quad (12)$$

where $m_2 = 3$, $e^h_1 = e^h_{WM}$, $e^h_2 = e^h_{DW}$, and $e^h_3 = e^h_{EV}$ are power consumptions of flexible loads including WM, DW, and EV at the hth hour, respectively.

B. Market Model

A model for retail markets may also be included in order to investigate the efficiency of the proposed DADRS. One main goal could be the encouragement of end users to distribute their demand in the non-peak periods. In the IBR modeling the marginal prices are increased by growing electrical consumption of users. Thus, the DAP with the IBR model could be employed for the retail electricity market. Benefits of the DAP with IBR model are:

- Investment cost is reduced because of no need to the advanced technologies.
- Households' consumptions are shifted to different times of a day, paying less to aggregators or retailers. Hence, the peak to average ratio is reduced for the load profile.
- It would be hard for the users to manage loads in various suggested market. However, users are able to schedule the operation of their flexible appliances among easily under the DAP with the IBR. Moreover, managing home appliances requires less investment with the DAP with the IBR compared to other market models.

In practice, retail marginal prices are sent to the aggregator according to Table IV, where the DAP of retail market will be released to the end users using a digital or manual communication infrastructure (e.g., internet or telephone). Therefore, total electricity cost of a residential unit at the hth hour is worked out as follows:

$$C^h = c^n(E^h_{Total}).E^h_{Total} \quad (13)$$

where c^n denotes a marginal pricing related to total demand at the h hour, E^h_{Total} and C^h are the total energy consumption of the residential unit and the end user payment at the hth hour, respectively. Table V shows a typical 12- level tariff rate structure

TABLE IV
DAP WITH THE IBR MODEL FOR RETAIL MARKETS

Energy consumption (W)	Price (Cents/kWh)
0- P_1	c^1
P_1-P_2	c^2
P_2-P_3	c^3
⋮	⋮
P_{n-1}-P_n	c^n

TABLE V
TYPICAL EXAMPLE GIVEN IN [24]FOR THE DAP WITH THE IBR IMPLEMENTED IN THE RETAIL MARKET

Power supply (W)	Price (Cents/kWh)	Power supply (W)	Price (Cents/kWh)
0-100	4.2	750-900	28.56
100-200	5.8	900-1000	38.5
200-300	8.75	1000-1150	52.5
300-400	15.75	1150-1400	63
400-500	18.06	1400-1600	87.5
500-750	22.75	>1600	91.8

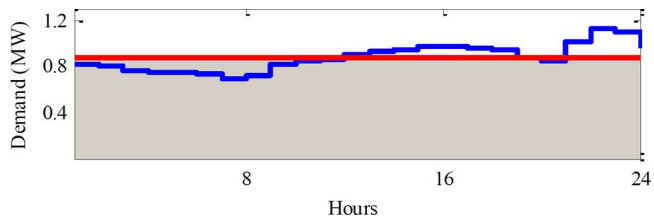

Fig. 7. Daily load profile of a typical aggregator for 100 residential units, where the red line is the optimal consumption pattern and the blue line is the typical load profile.

for the DAP with the IBR introduced in [23]. Marginal pricing of each level over the marginal pricing of its previous level is called marginal price factor (MPF). This paper uses Table V to examine the performance of the proposed DADRS.

C. Objective Function

The goal of this research is to propose a DADRS in order to reduce the peak demand as well as cost of the user in the retail market. Ideally, it is desired that the typical load profile of a sample feeder in the distribution system (blue line in Fig. 7) turns into a flat profile (red line in Fig. 7). Thus, the total consumed energy by the two profiles is equal, i.e., the gray area for the flat profile and the area under the blue load profile are identical. Hence, the peak demand would be optimally reduced. Therefore, this paper concentrates on moving the typical load profile (blue line) toward the optimal one (red line) by controlling flexible loads of residential units.

To establish the objective function, assume a residential unit purchases electrical energy from an aggregator according to the DAP with IBR model. Then, the following steps should be taken to form the objective function:

1) Using (6), (7), and (12), the total hourly energy consumption of a residential unit E^h_{Total} is expressed as

$$E^h_{Total} = te^h_{ASTOU}\left(e^{h,s_{A_1}}_1, e^{h,s_{A_2}}_2, \ldots, e^{h,s_{Am_0}}_{m_0}\right) +$$

$$te^h_{wl}\left(e^{h,s_{W_1}}_1, e^{h,s_{W_2}}_2, \ldots, e^{h,s_{W_{m_1}}}_{m_1}\right) + te^h_{TDR}. \quad (14)$$

2) Using (6) and (8), the average daily consumption in different scenarios (E^{ave}_h) can be expressed as

$$E^{ave}_h = \left(\frac{\sum_{h=1}^{24} te^h_{TDR}}{24} + E^{ave,s_{Wk}}_k + E^{ave,s_{Az}}_z\right). \quad (15)$$

3) Considering (13), the total daily energy cost of a residential customer can be summated as follows:

$$C_{Total} = \sum_{h=1}^{24}\left[c^n \times E^h_{Total}\right]. \quad (16)$$

4) A residential payment is minimized when the hourly energy consumption during 24 h remains identical to E^{ave}_h. This can be expressed in mathematical terms using (16):

$$\frac{\partial C_{Total}}{\partial E^1_{Total}} = \frac{\partial C_{Total}}{\partial E^2_{Total}} = \cdots = \frac{\partial C_{Total}}{\partial E^h_{Total}}. \quad (17)$$

5) Satisfying (17) together with minimizing (16) would result in minimization of the difference between blue and red lines in 24 h (see Fig. 7). In other words, the objective function is expressed as

$$\min \sum_{h=1}^{24}(E^h_{Total} \times (1\text{ hour}) - E^{ave}_h)^2. \quad (18)$$

It should be noted that the proposed objective function (18) introduces the proposed DADRS based on multivariate uncertainty analysis using the multivariate GC, in order to schedule flexible loads.

IV. Case Study and Discussions

Here it is introduced a case study that works on the collected exact data from residential loads with uncertainty over 50 days, including TV, PC, lighting, and AC. Then, the aforementioned generation of various scenarios for the ASTOU and WRL are applied to the exact data, where eventually the optimized scenario is singled out to manage flexible loads (WM, DW, and EV) in a residential unit.

A. Loads With Uncertainty

Two types of loads with uncertainty are considered in the case study; the ASTOU and the WRL.

1) The ASTOU: In this case study, lighting, PC, and TV are considered as the ASTOU, where their maximum demands are 400 W, 300 W, and 250 W, respectively. Empirical data show that a PC is often turned on once a day on average. Thus, two parameters are required to model the load profile of the PC; first, time of turning the PC on and the usage time after turning it on. These parameters were taken sample for fifty days as shown in Fig. 8(a). Then, the estimated **ECV** of the PC were simulated for 1000 different scenarios as shown in Fig. 8(b) using the bivariate GC $(m = 2)$. Similar procedure was repeated for both lighting and TV.

2) WRL: Various scenarios of the hourly temperatures were defined by dividing each day into 24 temperatures related to 24 h. Each temperature, as shown in Fig. 9 by θ^j_i, denotes the temperature at the ith hour in the jth day. Then, 24 temperatures in

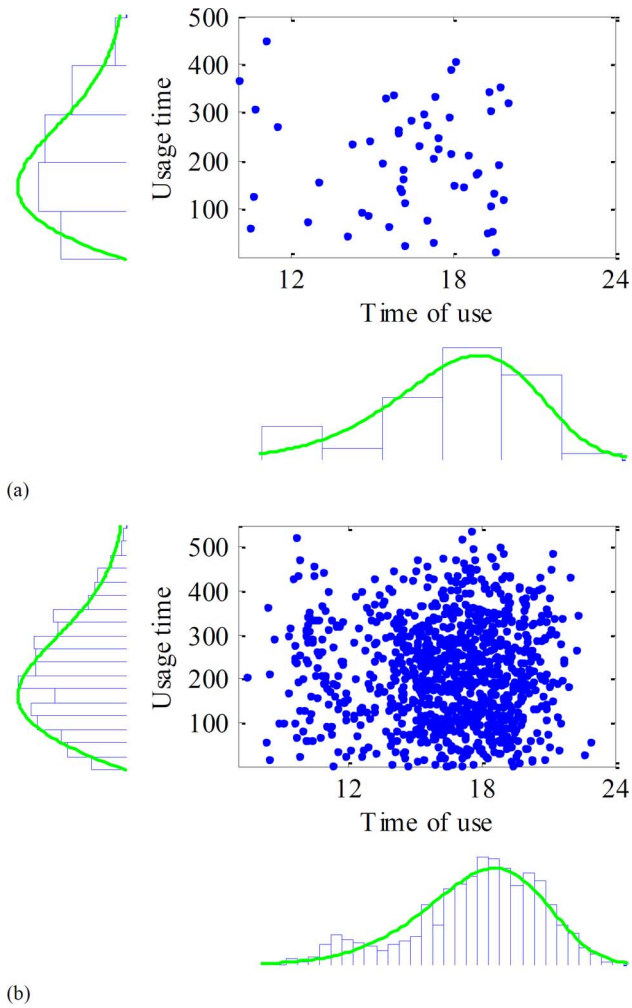

Fig. 8. Scatter plot for usage time versus time of use for a PC: (a) actual data for 50 selected days [time of use (mean $= 16.48$, variance $= 5.95$) and usage time (mean 200, variance $= 12539$)], and (b) simulated scenarios generated using the GC [time of use (mean $= 16.51$, variance $= 7.46$) and usage time (mean 216, variance $= 13865$)].

θ^j_1	θ^j_2	...	θ^j_i	...	θ^j_{23}	θ^j_{24}

Fig. 9. General form of hourly temperature in a day.

Fig. 9 were collected for fifty days which were close to the next day from the historical data in recent years. This was fed to a 24 variables GC. Simulations show that if the next day under estimation is May 19, then hourly temperatures from May 3 to May 18 in recent years are suggested for collecting the historical data. Further, 24 variables of the GC are related to 24 hours of a day, which their dependencies determine the parameters of the multivariate GC (**Rho**). The parameter **Rho** was calculated, which are listed in Table VI. It can be seen that the hourly temperatures in a day are correlated with each other based on the obtained **Rho**.

Assume the proposed stochastic DADRS is applied to a residential unit on May 19, 2011. Parameters of this residential unit are $\eta = 2.5$ and $\varepsilon = 0.938$ based on ($t_m = 6.3$ and $TC = 0.4$).

TABLE VI
COEFFICIENT MATRIX, **RHO**, FOR THE 24-VARIABLE GC ($M = 24$)

	u_1	u_2	u_3	u_4	u_5	u_6	u_7	u_8	u_9	u_{10}	u_{11}	u_{12}	u_{13}	u_{14}	u_{15}	u_{16}	u_{17}	u_{18}	u_{19}	u_{20}	u_{21}	u_{22}	u_{23}	u_{24}
u_1	1	0.9	0.66	0.42	0.49	0.53	0.92	0.57	0.76	0.78	0.73	0.66	0.68	0.69	0.8	0.72	0.69	0.69	0.73	0.66	0.61	0.63	0.65	0.66
u_2	0.9	1	0.74	0.45	0.53	0.62	0.87	0.63	0.75	0.76	0.72	0.68	0.69	0.7	0.8	0.72	0.74	0.69	0.75	0.71	0.63	0.66	0.67	0.71
u_3	0.66	0.74	1	0.79	0.76	0.75	0.63	0.93	0.5	0.54	0.64	0.7	0.65	0.69	0.58	0.66	0.49	0.47	0.68	0.75	0.68	0.6	0.4	0.72
u_4	0.42	0.45	0.79	1	0.9	0.76	0.48	0.91	0.36	0.44	0.58	0.68	0.68	0.69	0.45	0.63	0.3	0.28	0.48	0.66	0.69	0.61	0.25	0.61
u_5	0.49	0.53	0.76	0.9	1	0.86	0.6	0.86	0.38	0.46	0.61	0.67	0.72	0.69	0.48	0.64	0.3	0.35	0.55	0.71	0.73	0.66	0.26	0.67
u_6	0.53	0.62	0.75	0.76	0.86	1	0.64	0.81	0.43	0.49	0.58	0.65	0.7	0.68	0.51	0.63	0.44	0.45	0.62	0.68	0.7	0.67	0.37	0.68
u_7	0.92	0.87	0.63	0.48	0.6	0.64	1	0.57	0.71	0.75	0.73	0.66	0.73	0.7	0.78	0.72	0.61	0.63	0.64	0.62	0.59	0.61	0.59	0.62
u_8	0.57	0.63	0.93	0.91	0.86	0.81	0.57	1	0.42	0.5	0.62	0.71	0.67	0.71	0.52	0.66	0.41	0.39	0.64	0.74	0.73	0.65	0.34	0.71
u_9	0.76	0.75	0.5	0.36	0.38	0.43	0.71	0.42	1	0.92	0.78	0.72	0.75	0.73	0.95	0.76	0.83	0.77	0.68	0.65	0.6	0.7	0.81	0.65
u_{10}	0.78	0.76	0.54	0.44	0.46	0.49	0.75	0.5	0.92	1	0.9	0.79	0.82	0.81	0.95	0.86	0.76	0.73	0.71	0.67	0.65	0.72	0.75	0.66
u_{11}	0.73	0.72	0.64	0.58	0.61	0.58	0.73	0.62	0.78	0.9	1	0.89	0.89	0.87	0.83	0.94	0.64	0.6	0.71	0.73	0.76	0.77	0.59	0.72
u_{12}	0.66	0.68	0.7	0.68	0.67	0.65	0.66	0.71	0.72	0.79	0.89	1	0.91	0.91	0.78	0.97	0.57	0.5	0.69	0.78	0.83	0.81	0.49	0.76
u_{13}	0.68	0.69	0.65	0.68	0.72	0.7	0.73	0.67	0.75	0.82	0.89	0.91	1	0.92	0.8	0.9	0.63	0.61	0.73	0.79	0.82	0.84	0.59	0.79
u_{14}	0.69	0.7	0.69	0.69	0.69	0.68	0.7	0.71	0.73	0.81	0.87	0.91	0.92	1	0.78	0.9	0.63	0.62	0.74	0.8	0.8	0.84	0.6	0.78
u_{15}	0.8	0.8	0.58	0.45	0.48	0.51	0.78	0.52	0.95	0.95	0.83	0.78	0.8	0.78	1	0.81	0.81	0.78	0.72	0.68	0.65	0.73	0.8	0.67
u_{16}	0.72	0.72	0.66	0.63	0.64	0.63	0.72	0.66	0.76	0.86	0.94	0.97	0.9	0.9	0.81	1	0.62	0.55	0.73	0.79	0.83	0.81	0.54	0.77
u_{17}	0.69	0.74	0.49	0.3	0.3	0.44	0.61	0.41	0.83	0.76	0.64	0.57	0.63	0.63	0.81	0.62	1	0.91	0.74	0.68	0.6	0.73	0.95	0.71
u_{18}	0.69	0.69	0.47	0.28	0.35	0.45	0.63	0.39	0.77	0.73	0.6	0.5	0.61	0.62	0.78	0.55	0.91	1	0.73	0.66	0.59	0.7	0.96	0.69
u_{19}	0.73	0.75	0.68	0.48	0.55	0.62	0.64	0.64	0.68	0.71	0.71	0.69	0.73	0.74	0.72	0.73	0.74	0.73	1	0.92	0.84	0.85	0.66	0.94
u_{20}	0.66	0.71	0.75	0.66	0.71	0.68	0.62	0.74	0.65	0.67	0.73	0.78	0.79	0.8	0.68	0.79	0.68	0.66	0.92	1	0.93	0.89	0.59	0.99
u_{21}	0.61	0.63	0.68	0.69	0.73	0.7	0.59	0.73	0.6	0.65	0.76	0.83	0.82	0.8	0.65	0.83	0.6	0.59	0.84	0.93	1	0.95	0.53	0.93
u_{22}	0.63	0.66	0.6	0.61	0.66	0.67	0.61	0.65	0.7	0.72	0.77	0.81	0.84	0.84	0.73	0.81	0.73	0.7	0.85	0.89	0.95	1	0.67	0.9
u_{23}	0.65	0.67	0.4	0.25	0.26	0.37	0.59	0.34	0.81	0.75	0.59	0.49	0.59	0.6	0.8	0.54	0.95	0.96	0.66	0.59	0.53	0.67	1	0.62
u_{24}	0.66	0.71	0.72	0.61	0.67	0.68	0.62	0.71	0.65	0.66	0.72	0.76	0.79	0.78	0.67	0.77	0.71	0.69	0.94	0.99	0.93	0.9	0.62	1

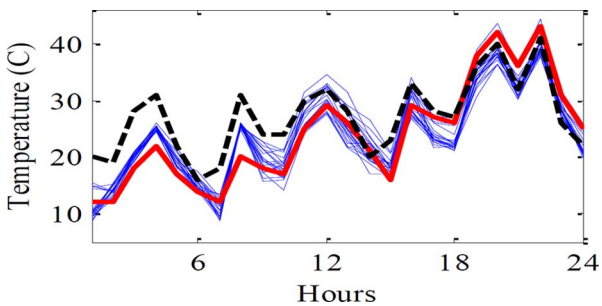

Fig. 10. Temperatures of 100 simulated scenarios on May 19, 2011.

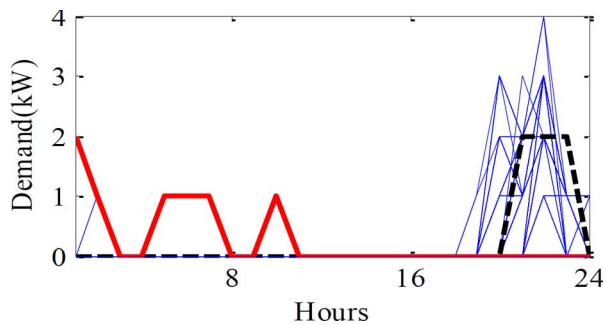

Fig. 11. AC energy consumptions for 100 simulated scenarios on May 19, 2011.

Hence, using the structure of Fig. 9, 100 scenarios were simulated using 24-variate GC (with the calculated **Rho**, shown in Table VI) for the hourly temperatures on May 19, 2011 as shown in Fig. 10. It was also considered 30% error for the collected hourly temperature prediction. Additionally, marginal distributions for 24 h in fifty days were used by the multivariate GC.

Fig. 10 illustrates actual hourly temperatures (dashed line), 100 simulated scenarios for hourly temperatures in blue and the hourly-predicted temperatures in red on May 19, 2011. The forecasting error, the difference between red and black curves, is 29.5% in line with the assumption considered in literatures (e.g., [23]).

In Fig. 11, the red line and dash black line illustrate the AC electrical consumption pattern [see (9)]according to the hourly predicted temperatures and actual hourly temperatures shown in Fig. 10, respectively; 100 blue lines in Fig. 11 show 100 hourly estimated energy consumption of the AC in the next day based on the hourly estimated temperatures (the blue lines in Fig. 11). However, $\theta_{\max}$ and $\theta_{\min}$ in (9) are controlled to be 25°C and 20°C, respectively. As it can be seen from Figs. 10 and 11, these 100 simulated scenarios (generated by the GC) have lower error compared to estimated temperature by the meteorological organization. Thus, it is expected to schedule flexible loads in the next day by the GC better than conventional approach.

B. *Flexible Loads*

It is necessary to have power consumption ratings and the time interval to plug in for flexible loads in order to schedule the DADRS in residential units. Table VII illustrates the DW, the WM and the EV along with their typical consumption energies. For example, the DW consumes 750 Watt-hour to clean breakfast dishes. Therefore, the total hourly demand for flexible loads in a residential unit is calculated according to (12).

C. *Studied Objective Function*

Here the proposed objective function (18) is specifically rearranged according to the studied consumptions of the uncertain

TABLE VII
FLEXIBLE APPLIANCES AND THEIR CONSUMPTION PATTERNS

Device type	Upper demand level (W)	Lower demand level (W)	Consumed energy (Wh)	Period of time to plug in
DW	**1000**	**0**	**1500 750 2000**	**[22-07] [09-13] [15-20]**
WM	**1000**	**0**	**3600**	**[01-24]**
EV	**1900**	**0**	**5000**	**[18-07]**

loads. Based on the stochastic process, it is aimed to satisfy the following objective function using (6) and (8):

$$\min \sum_{h=1}^{24} \Bigg[E_{Total}^{h} - \underbrace{\left(E_{TV}^{ave,s_{A1}} + E_{PC}^{ave,s_{A2}} + E_{Li}^{ave,s_{A3}}\right)}_{\text{ASTOU}} - \underbrace{\left(E_{AC}^{ave,s_{WA}}\right)}_{\text{WRL}} - \underbrace{\frac{1}{24}\sum_{h=1}^{24} te_{TDR}^{h}}_{\text{Flexible loads}} \Bigg]^{2}. \quad (19)$$

Here the flexible loads for the coming day could be pre-scheduled. Notice that E_{Total}^{h} in (19) can be concluded by using (14). The resultant objective function in (19) was programmed using MATLAB (linked with the GAMS). This link allows using programmed statistical modules of MATLAB to model all relationships among the ASTOU, which can be optimally scheduled for all flexible loads by the GAMS.

D. Simulations and Discussions

Fig. 12 illustrates simulations obtained from a residential unit that participated in the proposed DADRS. Black line in Fig. 12 shows the load profile excluding the DADRS which was collected from the actual data. Gray (dashed) line introduces the load profile including the proposed DADRS in (19) when both the ASTOU and the AC consumed demands were not modeled. Blue (dash-dot) line demonstrates the load profile including the proposed DADRS in (19) when both the ASTOU and the AC consumptions were modeled.

Fig. 13 depicts the consumed energy of various appliances in a residential unit. Fig. 13(a) shows the load profile for different appliances using the proposed DADRS with stochastic modeling of both the ASTOU and the AC. Fig. 13(b) illustrates those of Fig. 13(a) by excluding the simulated scenarios and Fig. 13(c) provides those of Fig. 13(a) by excluding the DADRS. Comparing these three pictures reveals that the energy cost of a residential unit decreased from \$4.73 (without the DR) to \$2.44 and \$1.78 per day when applying the proposed DADRS including and excluding the ASTOU and the AC models, respectively. Here MPF is equal to 1.2, resulting in about 48.4% and 62.4% reduction in energy cost for the third and fourth rows in Table VIII as well as around 31.1% and 47.26% drop in the daily peak demands. Table IX provides percentage of saving costs for different MPF. Simulations summarized in Tables X and XI confirm that the proposed DADRS satisfactorily reduces both costs and the peak demand of residential customers. Moreover, the efficiency of the proposed DADRS will be improved stochastic modeling is applied to the ASTOU and WRL.

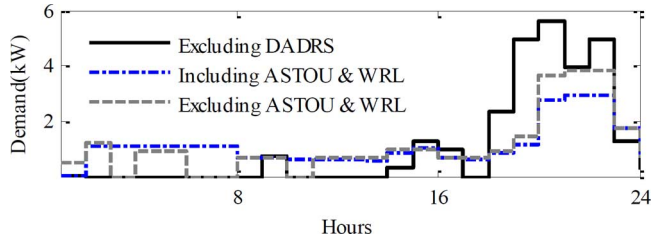

Fig. 12. Load profile for the participated residential units in the proposed DADRS.

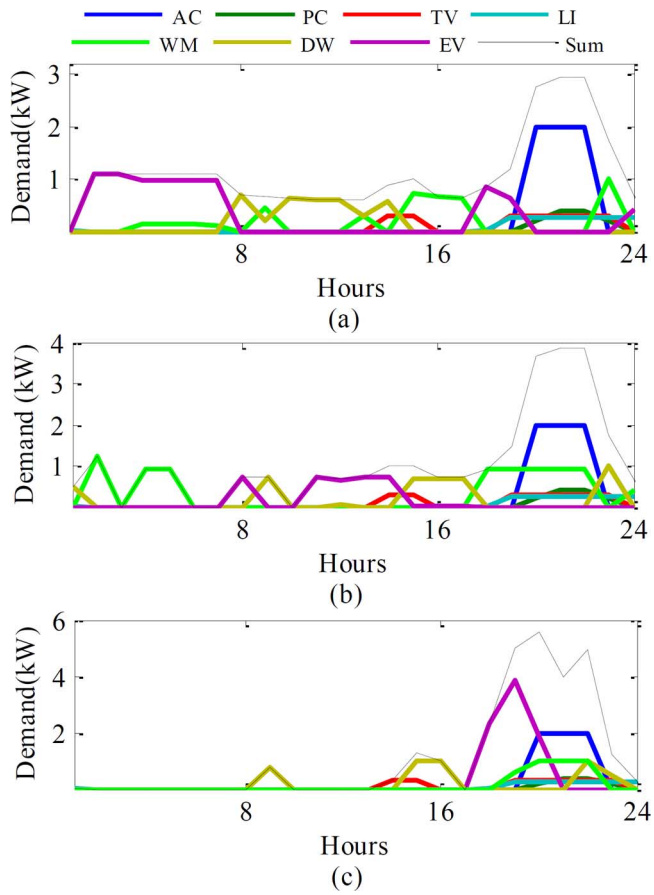

Fig. 13. Comparison of load profiles, (a) including the proposed DADRS through the simulated scenarios using the GC, (b) including the proposed DADRS excluding the simulated scenarios, and (c) excluding the DADRS.

TABLE VIII
END USER'S ELECTRICAL ENERGY COST (\$) UNDER THREE DIFFERENT TYPES OF FLEXIBLE LOADS MANAGEMENT

MPF	1.3	1.2	1.1	1.05
Excluding DADRS	9.78	4.73	2.24	1.54
Applying the proposed DADRS excluding ASTOU & AC	3.78	2.44	1.59	1.29
Applying the proposed DADRS including ASTOU & AC	2.31	1.78	1.37	1.21

The total demand is decomposed for each appliance from 19:00 until 22:00 (the peak period) as shown in Fig. 13. This

TABLE IX
ENERGY SAVING FIGURES BY ESTIMATING THE ASTOU AND WRL

MPF	1.3	1.2	1.1	1.05
Excluding ASTOU & AC	61.3%	48.4%	29%	16.2%
Including ASTOU & AC	76.4%	62.4%	38.8%	21.4%

TABLE X
ENERGY CONSUMPTION IN THE PEAK PERIOD ($[19:00-22:00]$) OF ALL APPLIANCES (IN FIG. 12) UNDER THREE DIFFERENT TYPES OF FLEXIBLE LOAD MANAGEMENT

	AC	ASTOU	EV	DW	WM	Sum
Excluding DADRS	6	3.2	5.68	1	3.6	19.48
Applying the proposed DADRS excluding ASTOU & AC	6	3.2	3.62	0	0	12.82
Applying the proposed DADRS including ASTOU & AC	6	3.2	0	0	0.621	9.821

TABLE XI
PERCENTAGE OF ENERGY SAVING (%) DURING THE PEAK PERIOD FOR ALL APPLIANCES (IN FIG. 12) UNDER THE TWO STUDIED DR CONDITIONS

	AC	ASTOU	EV	DW	WM	Sum
Applying the proposed DADRS excluding ASTOU & AC	0	0	36	100	100	34
Applying the proposed DADRS including ASTOU & AC	0	0	100	100	82	50

TABLE XII
SPECIFICATIONS IN THE USA MARKET (SEE [4]AND [37])

Model	**Battery capacity**	**Energy available**	**EV range**	**Max. Charge power rates**
GM-Ch. Volt	16 kWh	8 kWh	40 mi	240V 16A
Nissan-LEAF	24 kWh	19.2 kWh	100 mi	100V 30A
Volvo C30	24 kWh	22.7 kWh	93 mi	230V 16A
BMW MINI E	35 kWh	30 kWh	156 mi	240V 48A

compares the capability of the proposed models and the DR strategy for the day ahead DR by introducing the impact of each modeled equipment on reducing the peak of the load profile. Tables X and XI show the energy consumption and percentage of energy saving for each flexible load (EV, DW, and WM) as well as the ASTOU and the WRL, respectively. It can be seen that the energy consumption of the residential unit is decreased from 19.48 kW (without the DR) to 12.82 kW (excluding the model of ASTOU and WRL); this is further lowered to 9.82 kW when the proposed DADRS includes modeling the ASTOU (TV, PC and lighting) and the WRL (AC) at the peak period. Table XII lists the share of modeling both fixed and flexible loads on energy saving for the WRL, the ASTOU, the EV, the DW, and the WM in percent.

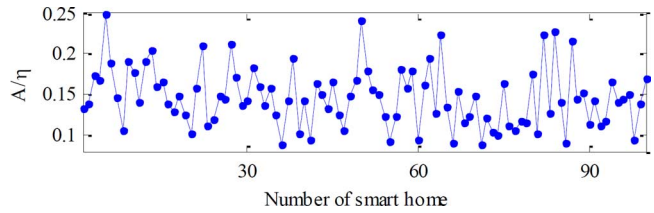

Fig. 14. Measured TC/η for 100 residential units.

Additionally, the load profile of 100 residential units was investigated to verify the proposed DADRS considering the uncertainty modeling. Every residential unit uses all the three categorized loads including an AC for the WRL, a WM (3.6 kWh), a DW (1.5 kWh for dinner, 0.75 kWh for breakfast, and 2 kWh for lunch), and an EV (see Table XII for EV ratings in the USA market [37]) for flexible loads and a TV (100 Wh~250 Wh), a PC (300 Wh~500 Wh), and lighting as the ASTOU. Their power range varies from 100 W for a TV up to 8~ 20 kW for an EV in each residential unit. To simulate the load profile, the following information on 100 residential units were required:

- For how long the EV were driven and when they were plugged in; it is assumed that all EV owners leave for work at different times (i.e., no parked EV is considered).
- The factor of inertia (ε) as well as the ratio TC/η which is shown in Fig. 14 for 100 households.
- The delivery time of cleaned dishes and clothes.

The above required data were collected through the distributed questionnaires among 100 residential units. Hence, households provided the required consumption bounds including the energy consumption region for each device along with their plug in and plug out times (e.g., for the WM and DW). Moreover, three scenarios are defined according to the battery charge data for the EVs listed in Table XII, with the following suggested combinations in penetration of different EV:

Scenario 1: Assume 100 EV include 34 Gm-Ch. Volt, 33 Nissan-LEAF and 33 Volvo C30; they were all usually plugged in at 6:00 pm, ready at 7:00 am on the next day.

Scenario 2: Assume 100 EV include 34 Gm-Ch. Volt, 33 Nissan-LEAF, and 33 Volvo C30; 80 out of 100 EV were usually plugged in at 6:00 pm, ready at 7:00 am on the next day. The remaining 20 EV were plugged in, staying at the state of being parked for 24 h.

Scenario 3: Assume 100 EVs are all of GM-Ch. Volt type.

The stated three scenarios were simulated for both including and excluding the DADRS. Fig. 15(a) shows 24-h-ahead load profile for 100 residential units including the WRL (in green), flexible loads (in blue), and the ASTOU (in red) without applying any DR strategies using the first and second scenarios. Fig. 15(b) considers the third scenario with the same characteristics as those of Fig. 15(a). Fig. 16(a)–(c) shows 24-h-ahead load profiles for 100 residential units including the WRL (in green), flexible loads (in blue), and the ASTOU (in red) with applying the DRDAS for the three scenarios. Comparing simulations in Fig. 15 with those of Fig. 16 confirms that the daily peak demands (for 100 residential units) were reduced by 41.85%, 45.92%, and 23.36% for the three scenarios, respectively.

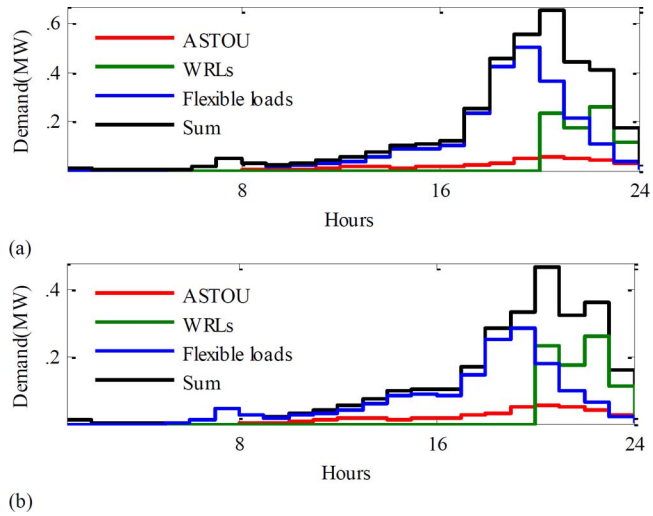

Fig. 15. Load profile for 100 residential units excluding the DADRS obtained by (a) the first and the second scenarios and (b) the third scenario.

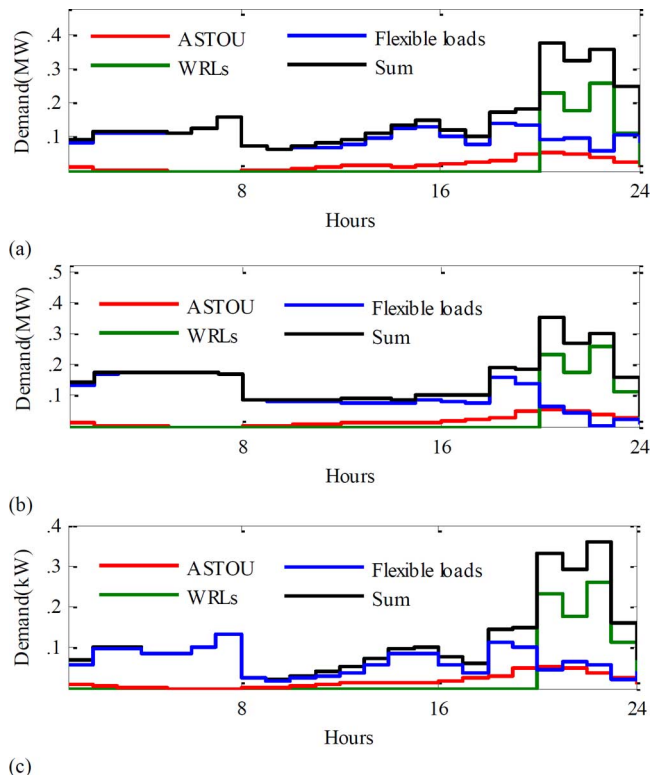

Fig. 16. Load profile for 100 residential units including the proposed DADRS based on stochastic modeling for (a) the first scenario, (b) the second scenario, and (c) the third scenario.

V. Conclusion

This paper is concentrating on a semi-automated home energy management system, proposing a practical strategy of the day ahead demand response. This can be applied to pre-schedule flexible loads in the next day. Thus, the energy consumption of the ASTOU and the WRL were both estimated based on the stochastic modeling, using the GC as a new efficient tool for the day ahead DR. Typical residential loads are classified into three named categories, where proper models are developed for a residential unit. Then, exact real collected data are fed to a copula function in order to correlate random variables and generate new data. Simulations show that the initial cost, the electrical energy cost of a household and the peak demand are reduced when the proposed DADRS is applied. Moreover, an aggregator is considered that feeds 100 residential units. These 100 units filled out the provided questioner to get the required data such as turning on times and their respected durations. Applying the DADRS to the prepared case for 100 residential units with three defined scenarios confirm that it can control flexible loads with the least influence on the customers lifestyle. Simulations also show that the proposed DADRS by applying the suggested models of the ASTOU and the WRL in scheduling flexible loads result in significant decrease not only in the users' costs but also in the peak demand for various load scenarios.

References

[1] S. Gyamfi, "Scenario analysis of residential DR at network peak periods," *Elect. Power Syst. Res.*, vol. 93, pp. 32–38, 2012.
[2] F. Partovi, "A stochastic security approach to energy and spinning reserve scheduling considering DR program," *Energy*, vol. 36, pp. 3130–3137, 2011.
[3] M. Marwan, "Demand side response to mitigate electrical peak demand in eastern and southern Australia," *Energy Procedia*, vol. 12, pp. 133–142, 2011.
[4] S. Shao, "DR as a load shaping tool in an intelligent grid with electric vehicles," *IEEE Trans. Smart Grid*, vol. 2, no. 4, pp. 624–631, Dec. 2011.
[5] N. Venkatesan, "Residential DR model and impact on voltage profile and losses of an electric distribution network," *Appl. Energy*, vol. 96, pp. 84–91, 2012.
[6] M. P. Somporn, "An algorithm for intelligent home energy management and DR analysis," *IEEE Trans. Smart Grid*, vol. 3, no. 4, pp. 2166–2173, 2012.
[7] E. Sortomme, "Optimal charging strategies for unidirectional vehicle-to-grid," *IEEE Trans. Smart Grid*, vol. 2, no. 1, pp. 131–138, Mar. 2011.
[8] A.-H. Mohsenian-Rad, "Optimal residential load control with price prediction in real-time electricity pricing environments," *IEEE Trans. Smart Grid*, vol. 1, no. 2, pp. 120–133, Sep. 2010.
[9] W.-C. Chu, "The competitive model based on the DR in the off-peak period for the Tai-Power system," *IEEE Trans. Ind. Applicat.*, vol. 44, no. 4, pp. 1303–1307, Jul./Aug. 2008.
[10] H.-G. Kwag, "Optimal combined scheduling of generation and DR with demand resource constraints," *Appl. Energy*, vol. 96, pp. 161–170, 2012.
[11] M. P. Moghaddam, "Flexible DR programs modeling in competitive electricity markets," *Appl. Energy*, vol. 88, pp. 3257–3269, 2011.
[12] P. Faria, "DR in electrical energy supply: An optimal real time pricing approach," *Energy*, vol. 36, pp. 5374–5384, 2011.
[13] I. Koutsopoulos and L. Tassiulas, "Optimal control policies for power demand scheduling in the smart grid," *IEEE J. Select. Areas Commun. (Smart Grid Series)*, vol. 30, pp. 1049–1060, Jul. 2012.
[14] S. Bashash and H. K. Fathy, "Modeling and control of aggregate air conditioning loads for robust renewable power management," *IEEE Trans. Control Syst. Technol.*, vol. 21, pp. 1318–1327, Jul. 2013.
[15] Y.-Y. Hong, "Multi-objective air-conditioning control considering fuzzy parameters using immune clonal selection programming," *IEEE Trans. Smart Grid*, vol. 3, no. 4, pp. 1603–1610, 2012.
[16] R. B. Nelsan, *An Introduction to Copulas*, 2nd ed. New York, NY, USA: Springer, 2006.
[17] T. Schmidt, "Copulas: From theory to applications in finance," in *Coping With Copulas*, J. Rank, Ed. London, U.K.: Risk Books, 2007.
[18] K. Goda, "Statistical modeling of joint probability distribution using copula: Application to peak and permanent displacement seismic demands," *Struct. Safety*, vol. 32, pp. 112–123, 2010.
[19] M. Farhadi and M. Farshad, "A fuzzy inference self-organizing-map based model for short term load forecasting," in *Proc. Elect. Power Distribution Networks (EPDC) Conf.*, May 2012, pp. 1–9.

[20] K. Goda, "Statistical modeling of joint probability distribution using copula: Application to peak and permanent displacement seismic demands," *Struct. Safety*, vol. 32, pp. 112–123, 2010.
[21] Help File for ModelRisk Version 4, Vose Software, 2007.
[22] A. Lojowska, D. Kurowicka, and G. Papaefthymiou, "Stochastic modeling of power demand due to EVs using copula," *IEEE Trans. Power Syst.*, vol. 27, no. 4, pp. 1960–1968, Nov. 2012.
[23] A. Sabziparvar and H. Tabari, "The estimated average daily soil temperature at a few examples of climate using weather data," *J. Soil Water Sci. Isfehan Univ. Technol.*, vol. 14, no. 52, pp. 125–138, 2010.
[24] D. Ahmadi and M. T. Bina, "Modeling and estimating the energy consumption of household electrical equipment having stochastic time of use using Gaussian copula," in *Proc. 27th Int. Power System Conf. (PSC'12)*, 2012.
[25] S. Shao, "Grid integration of electric vehicles and DR with customer choice," *IEEE Trans. Smart Grid*, vol. 3, no. 1, pp. 543–550, Mar. 2012.
[26] D. Chen and D. W. Bunn, "Analysis of the nonlinear response of electricity prices to fundamental and strategic factors," *IEEE Trans. Power Syst.*, vol. 25, no. 2, pp. 595–606, May 2010.
[27] C.-L. Su, "Quantifying the effect of DR on electricity markets," *IEEE Trans. Power Syst.*, vol. 24, no. 3, pp. 1199–1207, Aug. 2009.
[28] G. Koutitas, "Control of flexible smart devices in the smart grid," *IEEE Trans. Smart Grid*, vol. 3, no. 3, pp. 1333–1343, Sep. 2012.
[29] D.-M. Kim, "Design of emergency DR program using analytic hierarchy process," *IEEE Trans. Smart Grid*, vol. 3, no. 2, pp. 635–644, Jun. 2012.
[30] O. Corradi, "Controlling electricity consumption by forecasting its response to varying prices," *IEEE Trans. Power Syst.*, vol. 28, no. 1, pp. 421–429, Feb. 2013.
[31] M. Joung, "Assessing DR and smart metering impacts on long-term electricity market prices and system reliability," *Appl. Energy*, vol. 101, pp. 441–448, Jan. 2013.
[32] F. Javed, "Forecasting for DR in smart grids: An analysis on use of anthropologic and structural data and short term multiple loads forecasting," *Appl. Energy*, vol. 96, pp. 150–160, 2012.
[33] O. Sezgen, "Option value of electricity DR," *Energy*, vol. 32, pp. 108–119, 2007.
[34] M. Alcázar-Ortega, "Methodology for validating technical tools to assess customer DR: application to a commercial customer," *Energy Convers. Manage.*, vol. 52, pp. 1507–1511, 2011.
[35] J. Moral-Carcedo, "Modeling the non-linear response of Spanish electricity demand to temperature variations," *Energy Econ.*, vol. 27, pp. 477–494, 2005.
[36] D. T. Nguyen, "Modeling load recovery impact for DR applications," *IEEE Trans. Power Syst.*, vol. 28, no. 2, pp. 1216–1225, May 2013.
[37] S. Shao, "Development of physical-based DR-enabled residential load models," *IEEE Trans. Power Syst.*, vol. 28, no. 2, pp. 607–614, May 2013.

M. Tavakoli Bina (S'98–M'01–SM'07) received the B.Sc. and M.Sc. degrees in power electronics and power system utility applications from the University of Tehran and Ferdowsi, Iran, in 1988 and 1991, respectively, and the Ph.D. degree from the University of Surrey, Guildford, U.K., in 2001.

From 1992 to 1997, he was a Lecturer working on power systems with the K. N. Toosi University of Technology, Tehran. He joined the Faculty of Electrical and Computer Engineering at K. N. Toosi University of Technology in 2001, where he is currently a Professor of electrical engineering and is engaged in teaching and conducting research in the area of power electronics and utility applications.

Danial Ahmadi was born in Tehran, Iran, in 1985. He received the B.Sc. and M.Sc. degrees in electrical engineering from the Zanjan University in 2007 and K. N. Toosi University of Technology in 2009. Currently, he is pursuing the Ph.D. degree at K. N. Toosi University of Technology.

He joined the Faculty of Electrical and Computer Engineering at Pooyesh institute of Education in 2012.